We are IntechOpen, the world's leading publisher of Open Access books
Built by scientists, for scientists

6,900
Open access books available

185,000
International authors and editors

200M
Downloads

154
Countries delivered to

Our authors are among the

TOP 1%
most cited scientists

12.2%
Contributors from top 500 universities

CLARIVATE ANALYTICS
BOOK CITATION INDEX
INDEXED

WEB OF SCIENCE™

Selection of our books indexed in the Book Citation Index
in Web of Science™ Core Collection (BKCI)

Interested in publishing with us?
Contact book.department@intechopen.com

Numbers displayed above are based on latest data collected.
For more information visit www.intechopen.com

Study of an Individual Air-Conditioning Energy-Saving Equipment

Nguyen Anh Tuan[1], Wu-Chieh Wu[1,2] and K-David Huang[1]
[1]Institute of Mechanical and Electrical Engineering,
National Taipei University of Technology, Taiwan
[2]Network Operations Laboratory,
Chunghwa Telecommunication Laboratories, Taiwan
Republic of China

1. Introduction

Room air-conditioning does not always meet the optimal desire for thermal comfort of occupants and energy-saving goals [1]. This is due to the following reasons:

It is well established that differences exist between individuals in required comfortable temperature for their own local environments. (ii) Traditional air conditioning airflow distribution can stagnate around furniture, lights, and partitions which mean that airflow is distributed without consideration for the occupants' comfort demands. (iii) air-conditioning airflow has been distributed without consideration of occupants' demands beyond setting temperature and fan speed to meet thermal comfort standards, such as Predicted Mean Votes (PMV) and Predicted Percentage of Dissatisfied (PPD) indices (ISO-7730 2005) [2]. It may be that the actual presence of occupants in the workplace is less than that was set up from the original air conditioning design. This causes serious waste of cooling load to the system through unnecessary runtime. (iv) The traditional air conditioning air supply unit is set high on the ceiling or wall, which means that much of the cool air proportionally much consumed by light fittings, walls, and other surrounding objects. Therefore, this increases the demand on energy supply. In response to these concerns, several personalized air-conditioning systems have been showed and it rightly remains a great attention in efforts to design more intelligent workplaces.

Cho and Kim [3] introduced a personal environment module (PEM), the PEM was studied as an alternative air-conditioning system for improving thermal comfort in workspaces. Compared to a typical under-floor air-conditioning system, the advantages of the PEM is more flexible and easier to control.

Zeng et al. [4] introduced personalized ventilation systems (PVSs), that allow each occupant to control their own thermal comfort provision, such as airflow direction and temperature. The perceived air quality of the PVS is superior to that of a conventional ventilation system with the same amount of supplied air.

Melikov [5] have systematic reviews on the performance of personalized ventilation (PV) and on human response to it. PV, in comparison with traditional ventilation, has two important advantages: (i) it has potential for improving the inhaled air quality, and (ii) each occupant is delegated the authority to optimise as well as control the temperature, the flow

rate, and the direction of supplied air according to their own preferences and to thermal comfort requirements.

Nielsen et al. [6, 7] studied a chair with integrated personalized ventilation for minimizing cross infection. The idea behind this PV system is to utilize the fact that the head or the body in natural contact with surfaces as mattresses, pillows, neck support pillows, headrest, clothing, blankets, walls, and those surfaces are designed also to be a supply opening of fresh air. The chair with integrated diffuser has proven to be a very efficient system to protect people from cross infection because clean air is supplied direct to the breathing zone. Effectiveness up to 95% can be reached, and the different systems have in general effectives larger than 50% to 80%. The flow rate to the system should be at a level of 10 l/s in most cases.

Niu et al. [8] investigated a chair-based PVS that can potentially be applied in theatres, cinemas, lecture halls, aircraft, and even offices. Perceived air quality improved greatly by serving cool air directly to the breathing zone. Feelings of irritation and local drafts could be eliminated by proper designs. Personalized air with a temperature below that of room air was able to bring "a cool head" and increased thermal comfort in comparison with traditional ventilation.

Schiavon et al. [9–11] studied the energy consumption of a PVS and energy saving strategies which can be used to control a PVS and to develop and test an index for evaluating the cooling fan efficiency in a laboratory. The potential saving of cooling energy elevated air speed was quantified by means of simulations using EnergyPlus software. Fifty-four cases covering six cities (Helsinky, Berlin, Bordeaux, Rome, Jerusalem, and Athens), three indoor environment categories, and three air velocities (< 0.2, 0.5, and 0.8 m/s) were simulated. Cooling energy savings in the range of 17–48% and a reduction of the maximum cooling power in the range of 10–28% have been obtained. The PVS may reduce the energy consumption substantially (up to 51%) compared to mixing ventilation when the control strategies are applied.

Yang et al. [12] showed a new type of PV in which the PV air terminal device (ATD) is mounted on the ceiling is developed. Thus, the personalized airflow spreads and has a target area which covers larger area of the occupant body. Thirty-two subjects performed normal office work and could choose to be exposed to four different PV airflow rates (4, 8, 12, and 16 L/s). The results showed that if PV airflow rate was increased or temperature was reduced inhaled air was perceived cooler and perceived air quality and air freshness improved. In a following paper Yang et al. [13] evaluated energy-saving potential of the ceiling mounted personalized ventilation (PV) system in conjunction with back ground mixing ventilation compared with mixing ventilation system alone and with mixing ventilation system when occupants are provided with individually controlled desk fans for generating additional air movement at each desk. Comparing with mixing ventilation plus desk fans, ceiling mounted personalized ventilation cannot only realize better cooling effect but also decrease the total energy consumption.

Faulkner et al. [14] studied the ability of two task/ambient conditioning (TAC) systems using air supplied from desk-mounted outlets to efficiently ventilate the breathing zone of heated manikins seated at desks. The TAC provided 100% outside air at a flow rate of 7 to 10 L s^{-1} per occupant. A high value of air change effectiveness (~1.3 to 1.9) was presented and high values of pollutant-removal efficiency (~1.2 to 1.6) were achieved.

In recently published designs, Huang et al. [15–17] adopted computational fluid dynamics (CFD) simulations and experimental measurements in a room with an airflow management technique to control airflow in the room to meet the demand for a regional steady-state temperature. A regional air-conditioning mechanism (RACM) system was constructed with

an air uptake and outlet that created airflow circulation cells in the seating area of an occupant. Those studies considered the change in distance between the inlet and outlet ports, port heights, and air-inlet velocity. Results showed that the RACM could successfully establish an individual thermal environment zone. Compared to traditional air-conditioning systems, the RACM is predicted to save energy.

Nomenclature			
d	diameter of RACM pipe, m	q_{wall}	thermal conductivity, W/m.K
g	gravitational acceleration, m/s^2	V	air velocity, m/s
h_1	inlet port height, m	T	air temperature, ^{o}C
h_2	outlet port height, m	T_{in}	air inlet temperature, ^{o}C
k	turbulent kinetic energy, m^2/s^2	t	time, s
L	length of RACM pipe, m	x, y	Cartesian coordinates
L_1	distance between inlet port and floor surface, m	φ_1	angle of inlet port, ^{o}
L_2	distance between outlet port and floor surface, m	φ_2	angle of outlet port, ^{o}
P_{out}	outlet vacuum pressure, Pa	ε	turbulent dissipation, m^2/s^3
PMV	predicted mean vote	η	temperature gradient, K/m
PPD	predicted percentage dissatisfied, %	*Subscripts*	
Q_{in}	cooling air supply flow rate, m^3/h	*oz*	occupied zone

This paper presents ten cases divided into two groups in order to study the effect of two parameters on the creation of the airflow circulation cell by using the CFD simulation: the cool air supply flow rate (Q_{in}) and outlet port position (L_2). Experimental platforms were set up to test the validity of a simulation model, and the tested results showed good agreement with simulation. Our simulation results showed that the airflow circulation cell was quite sensitive to changes in Q_{in} and L_2. In comparison with the conventional air-conditioning, the RACM could create a desirable thermal comfort zone and reduce energy consumption by as much as 91.6 %. In addition, the experimental study shows that the airflow circulation cell could be managed easily within the occupied zone no matter with or without the manikin object. These results could be helpful for designers and consultants with needed knowledge for design of RACM systems.

2. System analysis

RACM system is a personalized air conditioning system, which is integrated by main cooling air supply system (CASS), a blower fan, a regional air conditioning system, a sucker fan and two dampers, as shown in Fig. 1. The CASS supplies cooling air to the RACM by the blower fan. During operating process, the cooling air will channel through the damper, regulate the cooling air and activate the occupied zone to generate a comfortable zone according to the opening angle of damper. The cooling air will direct to the RACM, where the cooling air will exchange the heat with occupied zone in the room, after that the cooling air was sucked back to the main air conditioning by the sucker fan through the

outlet port with the aim of recycling the cooling air from the occupied zone. Therefore, the RACM can turn on an independent airflow circulation cell. It cannot only satisfy thermal comfort occupants' required, but also reduce much energy consumption for the cooling air supply system.
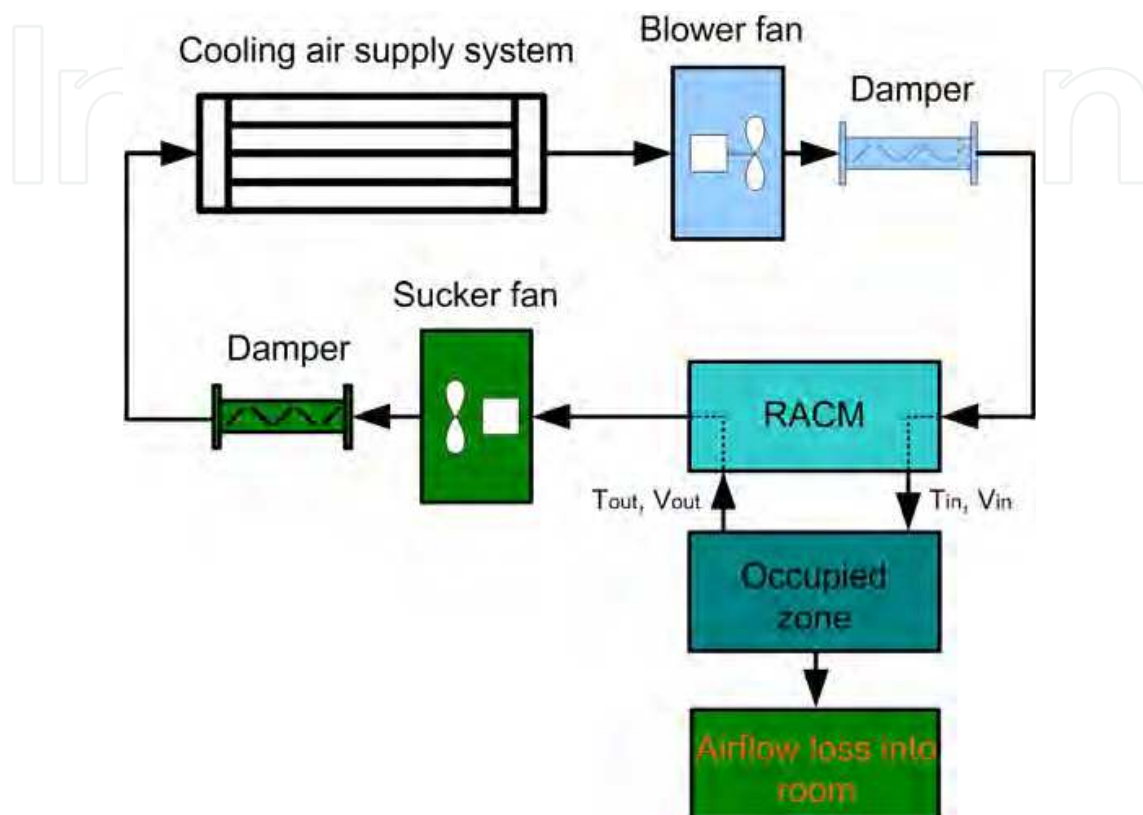

Fig. 1. Flow diagram of airflow in RACM system

3. Numerical method

3.1 Definition of model geometry and grid generation

An upper round part of the RACM has been designed for the air inlet and a lower round part has been designed for the air outlet on the main pipe of the RACM module as shown in Fig. 2. To improve the airflow distribution feature for space for human occupancy the adjustable louvers were fastened on inlet and outlet ports. The RACM enable the occupants to satisfy with respect to their own thermal comfort demands. The CFD code used in this study is FLUENT 6.3 [18]. The RACM was placed in the centre of the an empty workroom with no fixed furniture, nor occupants. Therefore, instead of using a 3D simulated model, a 2D one was applied in this study, as shown in Fig. 3. The 2D model workroom is the symmetrical two-dimensional (STD) model was described in detail in Huang's studies [15–17]. By using the solution-adaptive refinement such as gradient adaption of velocity, the initial STD model mesh can be refined by adding cells in occupied zone to enable the physical feature of the independent velocity field to be better resolved and coarsen in the rest of model room using GAMBIT software [19]. Therefore, the mesh quality of gradient adaption seems to better than initial mesh around occupied

zone of model. About 11555 nodes of triangular mesh are used in the STD model, thus, the gradient adaption has been chosen for further simulation.
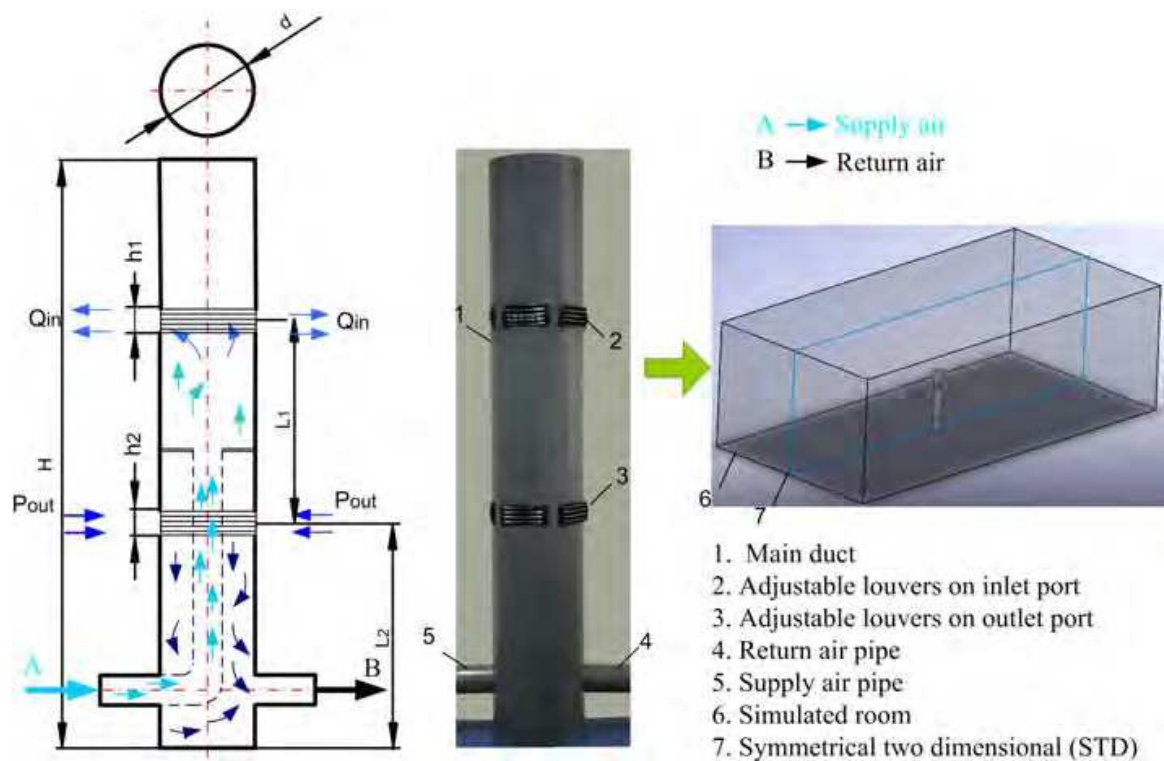

1. Main duct
2. Adjustable louvers on inlet port
3. Adjustable louvers on outlet port
4. Return air pipe
5. Supply air pipe
6. Simulated room
7. Symmetrical two dimensional (STD)

Fig. 2. Model of the regional air conditioning mechanism in the simulated room
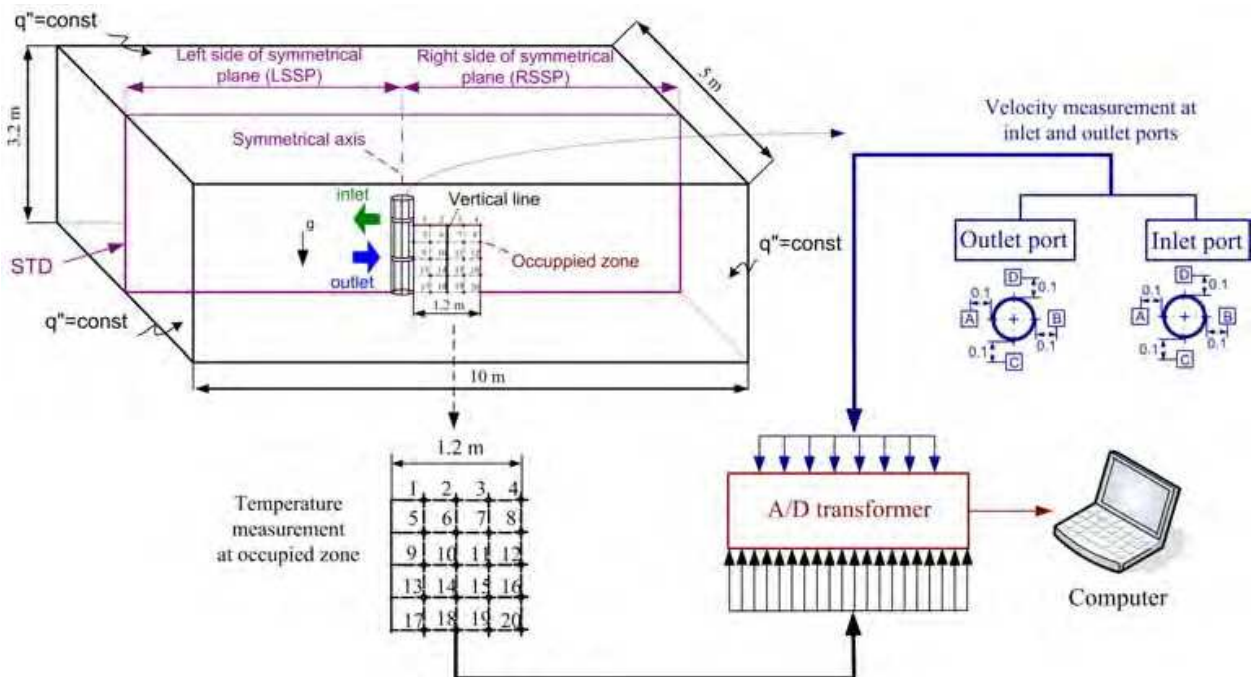
Fig. 3. Sketch layout of the RACM in the room

3.2 Simulation method

Assumptions are made with respect to the simulation of this study as follows:
The major assumptions of our analysis are as follows:

a. Newtonian fluid,
b. unsteady state,
c. effect of gravity and buoyancy are considered,
d. uniform air velocity at the inlet port,
e. standard $k - \varepsilon$ model is employed for modeling turbulent flow.

The following are the governing equations:
Continuity equation:
The mass conservation equation, or continuity equation, can be written as follows:

$$\frac{\partial p}{\partial t} + \frac{\partial}{\partial x_i}(\rho u_i) = S_m \tag{1}$$

Momentum equation:

$$\frac{\partial}{\partial t}(\rho \vec{v}) + \nabla p + \rho \vec{f} \tag{2}$$

Energy equation:

$$\frac{\partial}{\partial t}\left[\rho(e + \frac{\upsilon^2}{2})\right] + \nabla \cdot \left[\rho(e + \frac{\upsilon^2}{2})\vec{\upsilon}\right] = -\nabla \cdot (p\vec{v}) + \rho q + \rho(\vec{f} \cdot \vec{\upsilon}) \tag{3}$$

Where, t is the time, ρ is the mass density, υ is the flow velocity, p is the fluid pressure. The source S_m is the mass added to the continuous phase from the dispersed second phase and any user-defined sources, q is the heat transfer rate per unit area, e is the internal energy, and f is the body force.

The turbulence equation, which was proposed by Launder and Spalding (1974) to model the turbulent kinematics viscosity, is primarily related to the eddy viscosity [20].

3.3 Boundary conditions

The airflow equations were solved under the conditions for air inlet/outlet ports, and wall boundaries. The air supply flow rate (Q_{in}) and distance between floor surface and outlet port (L_2) were chosen for all ten cases, as shown in Table 1. The outlet vacuum pressure and the

Names	Q_{inlet} (m³/h)	L_2 (m)
Group 1	Changed from 20 to 110	0.5
Group 2	45	Changed from 0.1 to 0.9

Table 1. Calculation conditions

inlet air temperature for overall simulation were –2 Pa and 20 °C, respectively. Heat flux of vertical, ceiling, and a floor wall was 50 W m⁻². An adiabatic wall condition was chosen for the RACM walls and symmetrical axis. The surfaces of the walls of the room were assumed to have an emissivity ε of 0.85. The distance between inlet port and outlet port (L_1) was 0.6 m. RACM diameter (d) was 0.2 m. The inlet height port (h_1) was from 0.06 m to 0.1 m, outlet port height (h_2) was 0.06 m.

3.4 Validation of CFD simulations

The experiments were carried out in the Department of Mechanical and Electrical Engineering, National Taipei University of Technology. The schematic layout of the equipment and system used in this study is shown in Fig. 3. This system consists of a working room with the internal dimensions of $10m \times 5m \times 3.2m$ (ceiling height), a cooling air supply system, and an innovated RACM. The empty working room had an experimental temperature of 30 °C and a relative humidity of 50%. The study was conducted in Taipei, Taiwan during the summer, which is usually quite hot and humid. Detailed information about the equipment used in this study is shown in Table 2. Type-T thermocouple temperature sensors were set up at 20 points in the occupied zone to compare the experimental and simulation results, as shown in Fig. 3. A flow meter sensor was used for velocity measurement at four positions for both the inlet and outlet ports. Signals from temperature sensors and flow meter sensors were automatically transmitted to an A/D transformer and Testo−400 with recordings at 1 s intervals to ensure continuous reading by InstruNet and Comsoft-3 software running on a PC. All measurements were repeated at least three times at each test setting and the average experimental values of the three tests were considered to ensure stability and consistency.

Working room	$10m \times 5m \times 3.2m$
Cooling air supply system	2.7 kW–220 V
Diameter of RACM pipe	0.2 m
Total length of RACM pipe	1.7 m
Height of inlet and outlet ports	(0.06–0.1) m and 0.06 m
A/D transformer	InstruNet Model 100
Temperature sensor	(-40)–(+125) °C
Flow meter sensor	0–60 m/s
Computer	Joybook A52E

Table 2. Main component for the test RACM in the experimental setup.

3.4.1 Temperature at the occupied zone

The sensors at 20 points in the occupied zone were set up to compare in-room experimental and simulation results in the case of Q_{in} = 45 m³/h and L_2 = 0.5 m, as shown in Fig. 4. The simulation column shows trends similar to the experimental data column. The temperature difference between the simulation and experimental results was 0.18−1.38 °C in the occupied zone. It can be seen that the highest difference between the experimental and simulation results for temperature at the 20 points in the case of Q_{in} = 45 m³/h and L_2 = 0.5 m is about 4.7 %. Considering that the airflow is almost uncontrollable and natural, the simulation results of temperature in the occupied zone are in good agreement with the experimental data. Deviation at position 4 is larger than that of the other positions in the occupied zone presumably because the position is for the cooling air supply. On the other hand, part of the deviation may also be due to results from unsteady operation of the experiment.
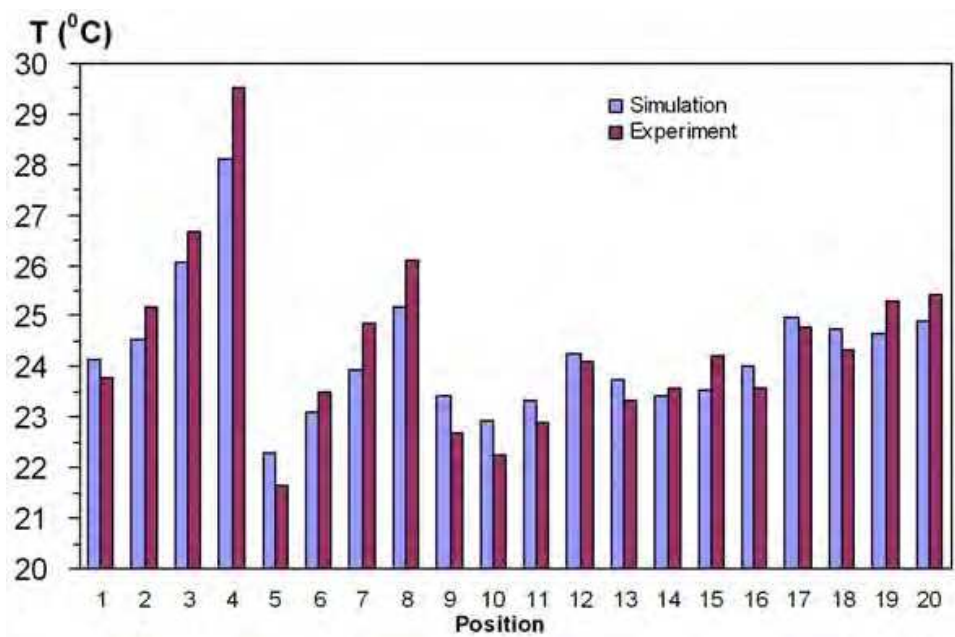
Fig. 4. Comparison of temperature between the experimental and simulation in the occupied zone of the room.

3.4.2 Velocity at inlet and outlet ports

Table 3 shows the comparisons of the experimental and simulation results of velocity for eight positions at the inlet and outlet ports under Q_{in} = 45 m³/h and L_2 = 0.5 m. The simulation and experimental results under the positions were good; however, it seems that the largest deviation is still large (~9.4 %).

In short, experimental and CFD data include the temperature and velocity in the occupied zone. The results of simulation are slightly different from the results of the experiments, around 9.4%. The fairly good agreement between experimental and simulation results indicates that the CFD simulation is possible to use in the investigation of in-room characteristics of the RACM.

Position	Experiment (m³/h)	Simulation (m³/h)
Air supply flow rate	44	45
Front inlet port		
Position A	0.212	0.234
Position B	0.25	0.248
Position C	0.231	0.245
Position D	0.213	0.225
Front outlet port		
Position A	0.172	0.181
Position B	0.161	0.168
Position C	0.172	0.181
Position D	0.152	0.165

Table 3. Comparison of velocities from experiment and simulation for the model room.

3.5 Calculus simulation

Based on the theory that the airflow convection effect is much stronger than the diffusion effect, this research aims to limit the air energy to a certain area by means of creating a circulation cell. The inlet airflow speed acts as the inertia, and the outlet vacuum pressure provides the centrifugal force required to form a circulation cell. In this manner, the RACM can create in the room a certain area that has the temperature different from the rest of the room. In this study, a total of two groups were simulated using FLUENT for a summer period. The room's internal dimensions were $10m \times 5m \times 3.2m$ as shown in Fig. 3. The left corner zone of the right side of symmetrical plane (RSSP) (length = 0.1–1.2 m; height = 0–1.4 m) corresponds to the occupied zone of the room as depicted in Fig. 3.

4. Results and discussion

4.1 CFD results

In this study, the RACM system was built based on the tested RACM in room with the length, diameter, and height of outlet port of pipe fixed, distance between inlet and outlet ports as constants. Nevertheless, the distance between floor surface and outlet port (ground effect distance) is adjusted with L_2 from 0.1 to 0.9 m. The height of inlet port of pipe are adjusted with h_1 from 0.06m to 0.1m.

4.1.1 Effect level of Q_{in} on establishing independent airflow cell process

The simulated results show the effect of the levels of Qin and L2 on the thermal comfort at occupied zone and energy saving potential. The RSSP is the important plane, since it represents the condition of the symmetrical plane well. The level effect of Q_{in} adjustment on establishing independent cell process in the case of $L_2 = 0.5$ m and the inlet velocity being adjusted from $Q_{in} = 20$ m³/h to 110 m³/h is presented in Fig. 5. Fig. 5 depicts the thermal environment on the RSSP after five hundred seconds of cooling. It is seen from Fig. 5 that

the air supply flow rate acts as the inertia and the outlet vacuum pressure provides the centrifugal force to form an independent airflow circulation cell well. Energy and concentration are kept well inside the cell. It is also observed from Fig. 5 that it can form the coolest region at the left corner zone of the RSSP in some of the studied cases. The airflow loss increases as inlet velocity increases, there is airflow changing to horizontal direction and moving further away from occupied zone that is the cause of making whole cooled room and consume much cooling load. The average air temperature and velocity in these zones is in the range of 22.1–24.4 °C and 0.21–0.34 m/s, respectively. These are the comfortable temperature and velocity magnitude for the occupant in mainly sedentary, activity during summer conditions [21].
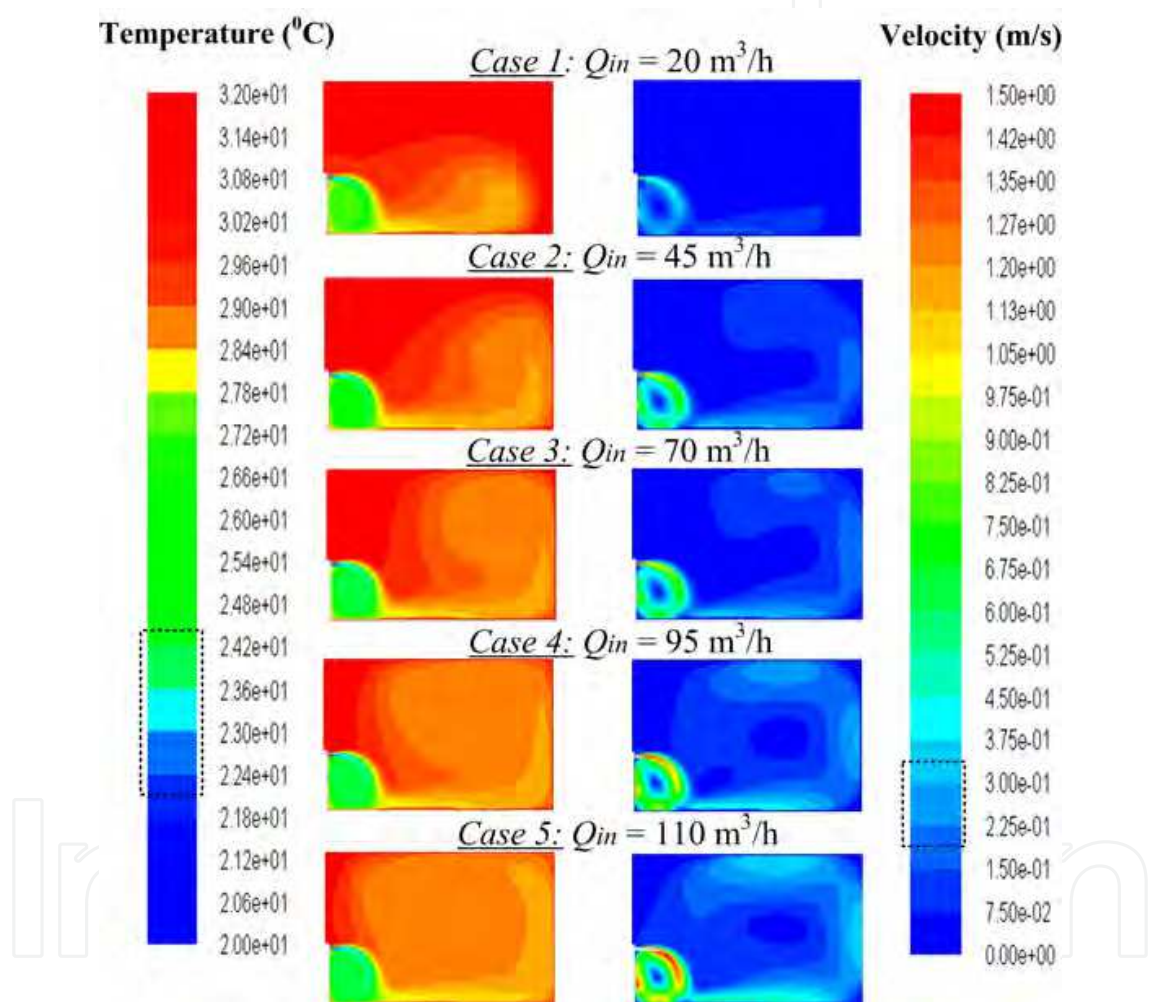
Fig. 5. Temperature and velocity distribution at the occupied zone of the room RSSP with different Q_{inlet} (L_2 = 0.5m).

4.1.2 Effect level of L_2 on establishing independent airflow cell process

The level of the ground effect adjustment on creating of the independent airflow circulation cell in the case under the Q_{in} = 45 m³/h and the ground effect distance being adjusted from the L_2 = 0.1 to 0.9 m is presented in Fig. 6. This figure shows clearly that the independent cell is significantly affected by the L_2 adjustment. With L_2 = 0.1 and 0.3 m, the independent cell at occupied zone is smaller than that of the case of L_2 = 0.5 m. The reason for this is that

presumably the cooling airflow entering the room travels shorter distance possible than that of L_2 = 0.5 m case before leaving the room. For the case of L_2 = 0.5 m the relative distance between room ground and outlet port is long enough to form a good independent cell that fills almost all of the occupied zone with just a small airflow loss that is located at the bottom surface. Going through the two cases of L_2 = 0.7 and 0.9 m of Fig. 6, one can observe the changes in the flow field where the position of the inlet port is higher than that of the L_2 = 0.5 m case along the RACM wall. In these cases, the area occupied by the independent airflow cell diminishes and the temperature distribution will increase to a larger area of the room as L_2 is increased. This is because of the fact that as the distance between floor surface and outlet port increases the ground effect is not strong enough to aid this cooling air inlet flows back to the outlet port. The mean velocity of the occupied zone varies from 0.19 m/s to about 0.27 m/s. The temperature in the same group varies between 22 °C to about 25.1 °C in the occupied zone. This indicates a temperature rise about 3.3 °C for the varied relative distance between room ground and outlet port. Therefore, the distribution patterns in Figs. 5 and 6 show that an independent airflow cell can be successfully established. The suitable adjustment of the L_2 for a better creating of the independent airflow cell was achieved in the occupied zone as the L_2 is 0.5 m.

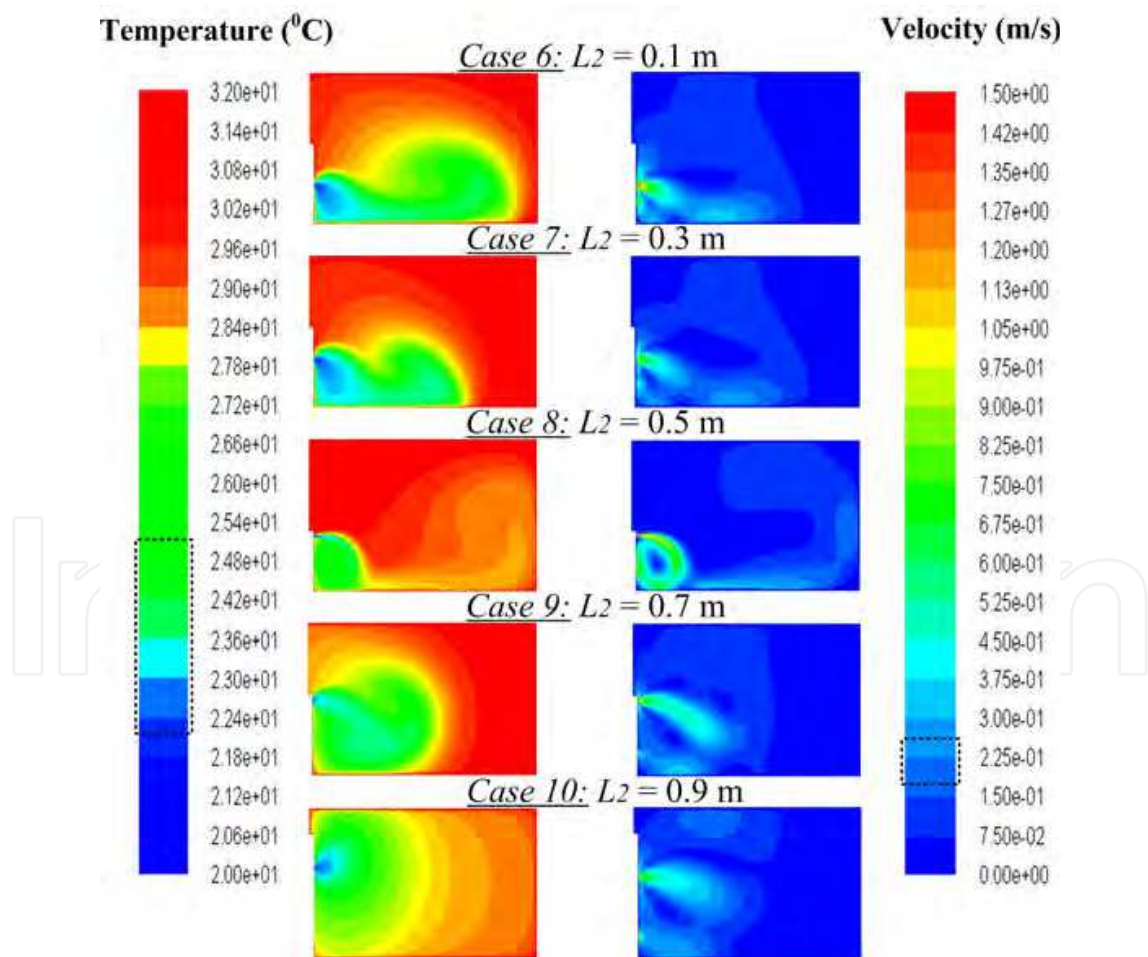Fig. 6. Temperature and velocity distribution at occupied zone of room with different L_2 (Q_{inlet} = 45 m³/h).

4.2 Thermal comfort indices

The thermal comfort of an occupied zone is an important issue. One method of assessing thermal comfort is to use the equations for predicted mean vote (PMV) proposed by Fanger [21, 22]. PMV is defined by six thermal variables of indoor air and conditions of human occupants: air velocity, air temperature, mean radiant temperature (MRT), relative humidity of the air, clothing, and physical activity. Figure 7 shows a combination of each thermal variable affecting PMV level. Fanger showed that values of PMV between −0.5 and +0.5 are in the range within which 90% of people are satisfied [21, 22]. The PMV corresponds to a prediction of the mean value of the votes of a large group of persons on the seven-point thermal sensation scale as shown in Fig.7.
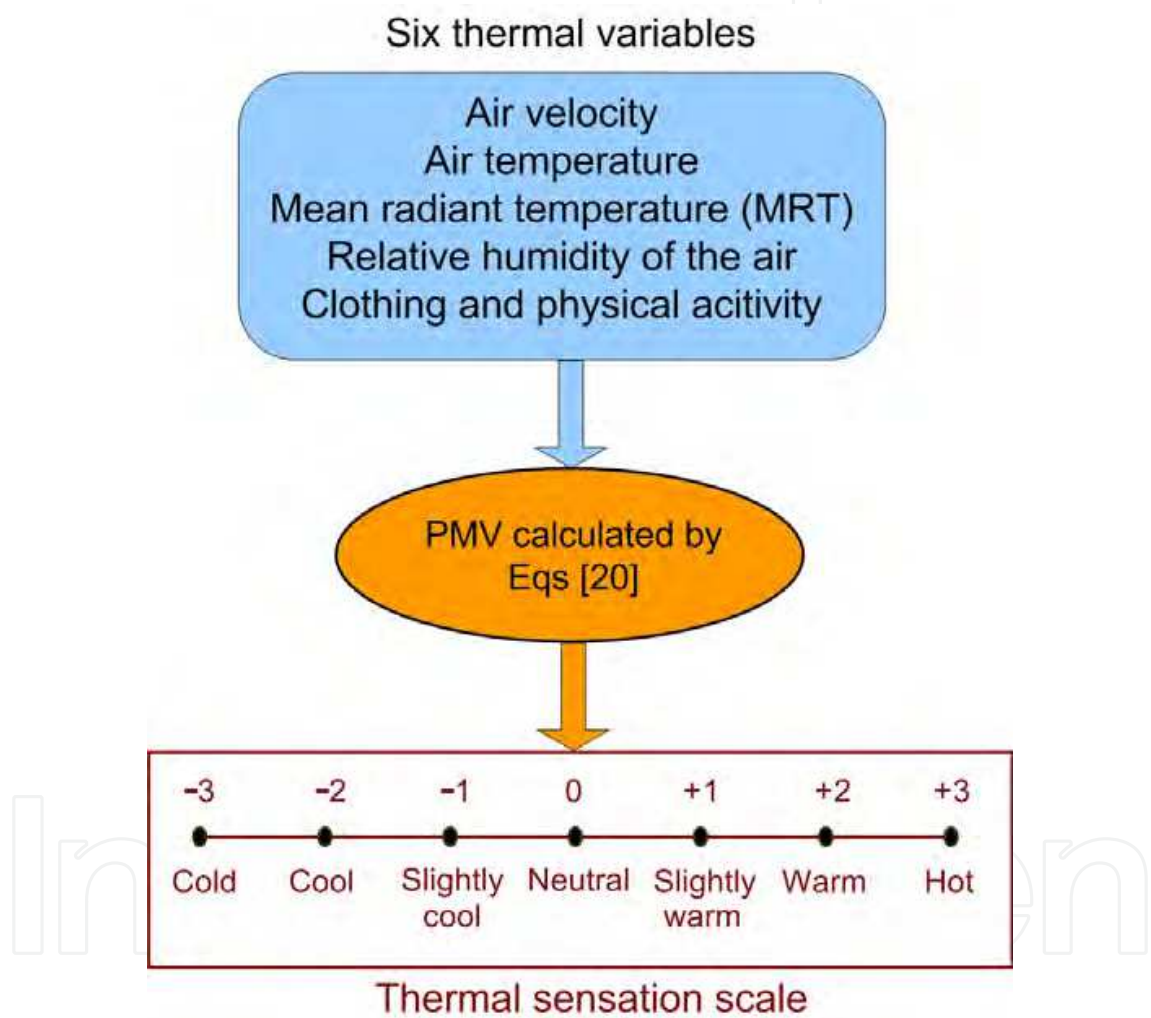
Fig. 7. Thermal comfort index.

The thermal comfort PMV index in this study was calculated by using parameters for cooling conditions in summer, mainly sedentary activity level −1.0 met and with a clothing thermal resistance of −0.5 clo. Relative humidity is assumed to be 50 % in the room, and MRT has been estimated using the P_1 radiation model [21, 22]. The overall thermal climate predicted by the PMV index can be seen in Fig. 8. It is seen from Fig. 8. that the PMV index is sensitive in air supply flow rate increase and various outlet positions. In group 1, case 5 has the worst PMV index among five cases, because the highest Q_{in} enters the room that

causes the occupied zone to become less comfortable. The case 2 with Q_{in} = 45 m³/h seems to offer higher PMV potential among five cases in group 1, it was therefore chosen to be investigated the effect of L_2 in this study. Moving on to the group 2, the PMV index in case 8 gives higher potential with L_2 = 0.5 m. When L_2 is 0.1 m in case 6, the cooling flow entering the room travels the shortest distance between the floor surface and the outlet port before leaving the room, therefore the airflow circulation cell is smaller than that of the rest cases, it may cause a lower PMV value in case 6. When L_2 is 0.9 m in case ten, the airflow circulation cell diminishes that causes the PMV potential decrease in occupied zone in the room. Case 8 seems to offer higher PMV potential in group 2. Therefore, it may be seen that if the parameters are set for the RACM system as in case 8, it will be the one among ten simulated cases in this study which offer the most thermal comfort.
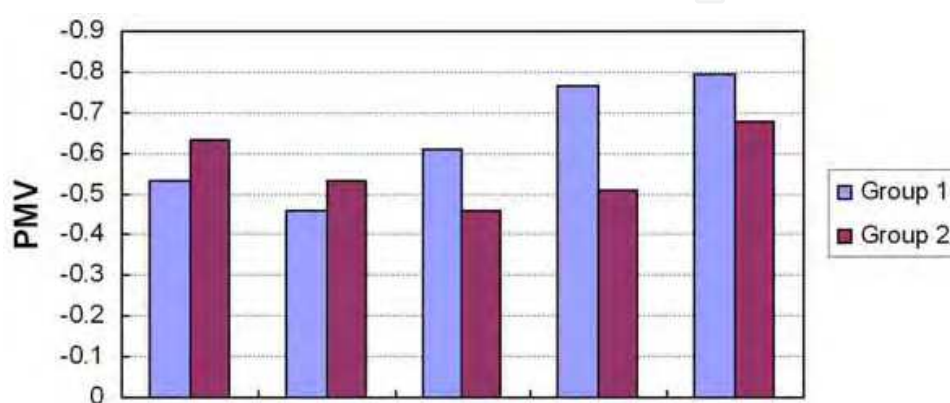
Fig. 8. PMV variation in the occupied zone

4.3 Vertical temperature profiles

The difference in the vertical air temperature between the feet and the head must be considered in determining conditions for acceptable thermal comfort. The vertical temperature profile is a function of sedentary occupant height. One measure indicates that the most comfortable thermal environment is achieved when the air temperature at head level is lower than the temperature of the floor surface [22]. It is worth noting that the difference of an allowable vertical temperature between 1.1 m and 0.1 m (head and ankle level) shall be less than 3 °C [22].

The predicted vertical temperatures were calculated for x is 0.6 m from the symmetrical axis as shown in Fig. 3 at different heights of 0, 0.1, 0.4, 0.6, 0.9 and 1.1 m from the floor surface level for all groups. These heights are assumed to represent the feet, ankle, knee, waist, shoulder, and the head of the occupant. It is obvious from Fig. 9 of group 1 that the difference for height from ankle (0.1 m) to the head level (1.1 m) is in the range of (−0.41 °C) – (−0.34 °C) the differences in vertical temperature are relatively low for all cases. Increasing Q_{in} leads relatively to the moving of air profiles to left hand side of Fig. 9. The reason for this is that, the inlet air flow rate increases, proportionally more flow blows into the room. For group 2, as the outlet port increases, the temperature profile up to head height is affected slightly in comparison to those in group 1 with the same physical parameter. The difference in temperature from the ankle to the head level is in the range of (−0.43 °C) – (−0.36 °C). It seen Fig. 9 that group 1 is the most sensitive from the point of view of varying air temperature profile along vertical line from surface to the head of the occupant as inlet air flow rate changes.
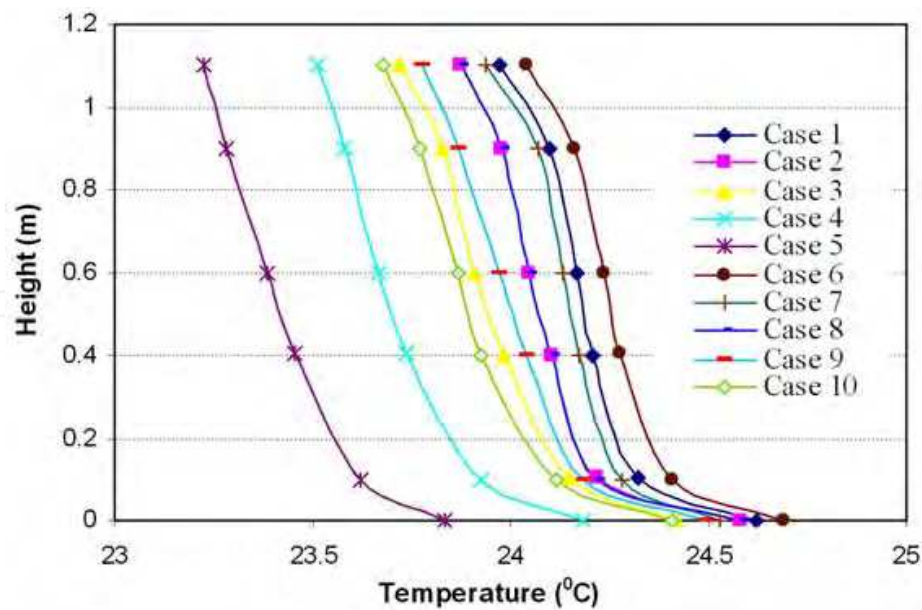
Fig. 9. Vertical temperature profile in the middle of the occupied zone

4.4 Energy-saving potential in a test case

In the case 2 study, Q_{in} = 45 m³/h. Inlet air temperature of 20 °C is blown from inlet port to the room. This supply continues for one hour, which makes 0.9 m³/h air supply rate for a 1 m² floor area. The difference between inlet and outlet temperatures, $\Delta T = 27 - 20 = 7$ K, is observed. The cooling capacity is then calculated as 2.1 W/m² using following formula:

$$\text{Cooling capacity} = (\dot{V}\rho)C_p\Delta T \qquad (6)$$

Where $\dot{V}$ is volume flow rate of the air (2.5.10⁻⁴ m³ s⁻¹), ρ is density of air (1.2 kg m⁻³), C_p is specific heat capacity of the air (1.10³ J kg⁻¹K⁻¹), and ΔT is the difference between the inlet and outlet air temperatures (7 K).

By means of a conventional air conditioning technique for a room three meters high, temperature difference $\Delta T = 9$ °C, the design temperature gradient $T_{1.1} - T_{0.1} = 3$ K m⁻¹ with an occupancy design air temperature of $T_{1.1} = 23$ °C. Temperature supply of $T_s = 17$ °C and the cooling capacity of 25 W m⁻² are given by Levermore [23]. Compared to conventional air-conditioning, supplying air at 17 °C, the RACM, supplying at 20 °C, will save on chiller energy. In fact, the free cooling obtained by using cool fresh air will contribute a considerable amount to the cooling, especially, in summer conditions. Traditional air conditioning typically maintains the room at an air temperature of 23 °C whereas RACM has a typical occupied zone temperature of 23.8 °C as shown in case 2 of Fig.5. so this technique also saves on thermal energy whereas it does not reduce comfort [23]. But cooling differentials also have to be considered. For conventional cooling, the differential is 23–17 = 5 °C and the RACM the differential is 23.81–24.22 = –0.349 °C as shown in case 2 of Fig.6. For the same heat load, the conventional system will require higher flow rates than the RACM in order to maintain air distribution uniformly in the whole room while the RACM just requires this for the occupied zone. The RACM can cope with about 2.1 W/m² whereas a conventional system can cope with more than 25 W/m², proportionally energy efficiency reduce 91.6 %, so the RACM will use considerably less energy.

4.5 Experimental test

The regional air conditioning system is designed to create the independent airflow circulation cell based on convection effect being much greater than the diffusion effect. The room is divided into region with separate temperature section around the RACM as predicted in Figs. 5 and 6. This is to be expected because the airflow from the high pressure area to the low pressure area, plus the inlet air that blows straight down and is sucked back to outlet port by the outlet vacuum pressure.

4.5.1 Comparisons of the measured thermocouple data

Air temperature was monitored at six locations in the measurement room, then compared during a 500-second cool-down experiment. As shown in Fig. 10, the six locations were placed on the RSSP. The measured thermal data for occupied and non-occupied zone (the middle and right corner of the RSSP) are shown in Figs. 11 and 12.
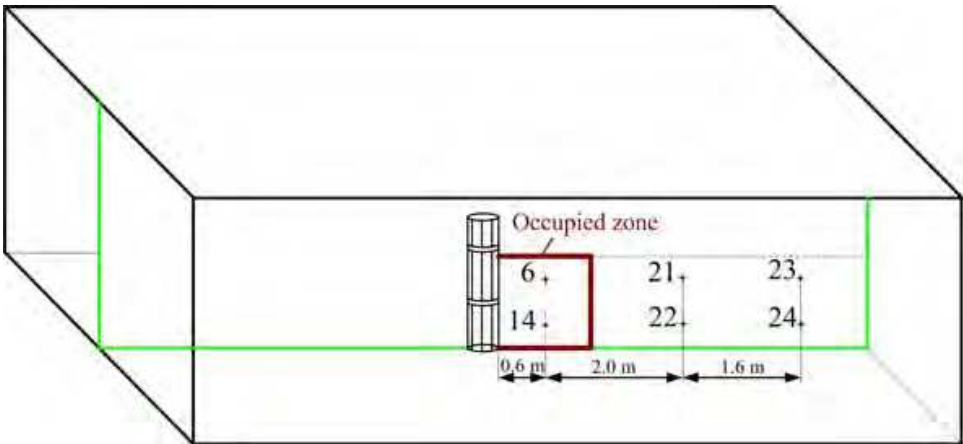
Fig. 10. The sketch of the eight monitored temperature locations in the RSSP
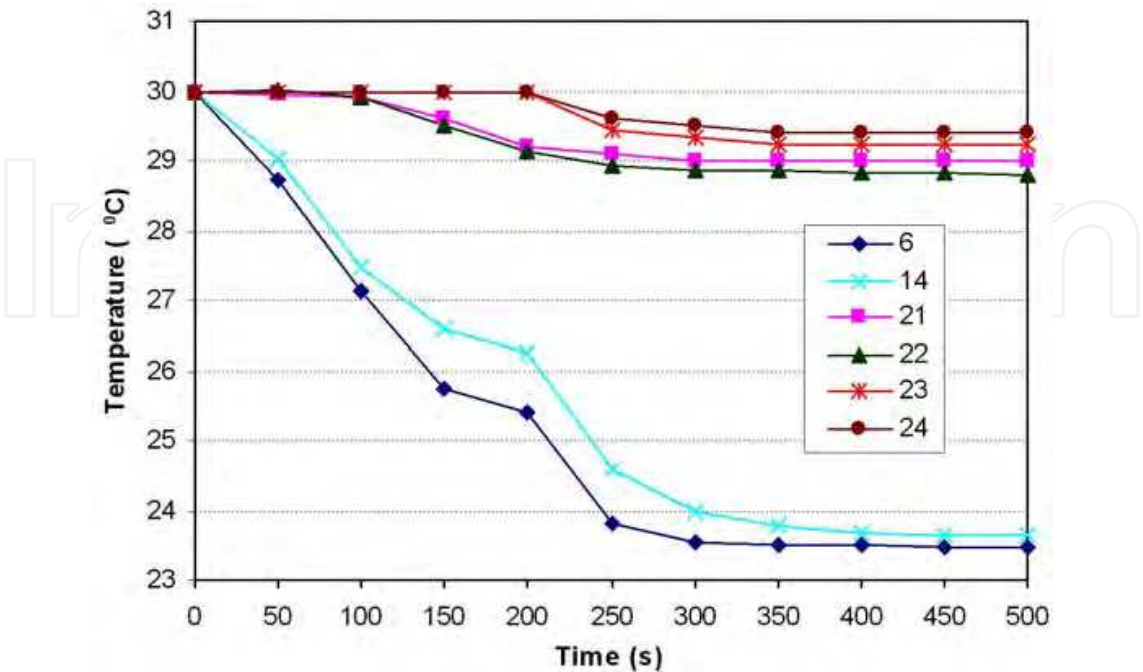

Fig. 11. Experimental temperature at six locations in the room (without a manikin)

4.5.2 Case I: Measurement without a manikin

Experiments were conducted in the initial room temperature of 30 $^{\circ}$C under the Q_{in} of 176 m³/h and the L_2 of 0.5 m. The temperature sensors were located at six positions as shown in Fig. 10, and then compared during a five hundred second cool-down experiment. Judging from the temperature field experiment as shown in Fig. 11, when the RACM is open, the system will run to maintain the occupied zone at a temperature around 23.5 $^{\circ}$C, the middle of the RSSP around 29 $^{\circ}$C, and the right corner of the RSSP around 29.5 $^{\circ}$C. With the temperature different between the occupied zone and the middle of the RSSP are up to 6 $^{\circ}$C and that at the right corner of RSSP are up to 5.5 $^{\circ}$C. The occupant can feel different temperatures, which means that the occupied zone temperature distribution has met the demand of regional air-conditioning. Thus, the airflow circulation cell was successfully created in the occupied zone.

4.5.3 Case II: Measurement with a manikin

The influence of a manikin is shown in Fig. 12. A manikin was placed in the occupied zone and the RACM was turned on at an inlet temperature preset to 20 $^{\circ}$C. The occupied zone temperature was from 24 to 24.5 $^{\circ}$C, as shown in Fig. 12. This result shows that the airflow circulation cell is barely affected by a manikin and the target region is still accurately controlled to the preset temperature range. However, other regions are influenced by conduction and radiation, resulting in a drop of 0.5−1 $^{\circ}$C to reach 29−30 $^{\circ}$C. Compared with Case I, temperature distributions in the occupied zone still met the low temperature. Its goal can make the room divided into two regions with separate temperature sections without any partitions.
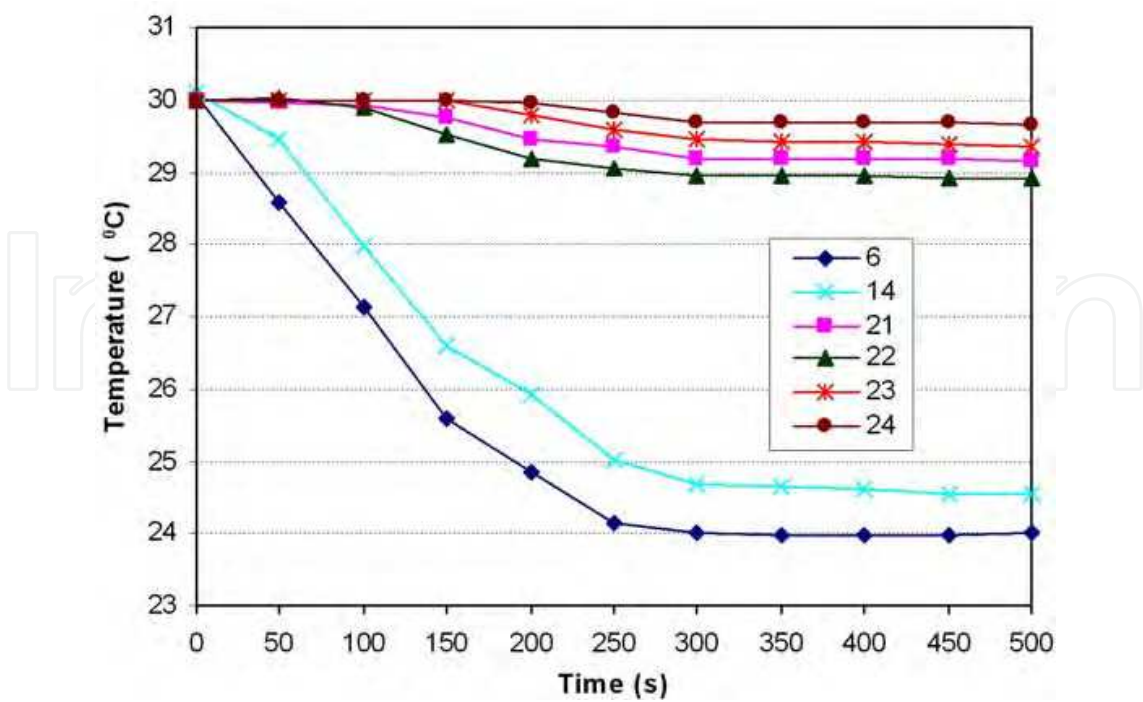

Fig. 12. Experimental temperature at six locations in the room (with manikin)

5. Conclusions

The present study introduces a new concept of energy saving mechanism design referred to as a regional air conditioning mechanism (RACM). Numerical predictions of distribution patterns in a room with this mechanism were conducted and reported. Experimental work was carried out to study the thermal regions of the RACM system. The results showed that:

i.   Air convection is dominant inside the cell; inter cell only air diffusion operates and there is no mixing effect. Since the convection effect of airflow is much stronger than diffusion, the energy and concentration can basically be kept inside the cell. Therefore, the regional air-conditioning mechanism can be successfully established.

ii. The parameters of the RACM, including Q_{in} and L_2, influenced thermal comfort in the occupied zone. This result is very helpful in showing the important impacts, which must be considered when designing the RACM system.

iii. Under suitable adjustments of Q_{in} = 45 m³/h and L_2 = 0.5 m, the highest level of thermal comfort demand can be achieved.

iv. The vertical temperature profiles in the middle of the occupied zone were almost uniform from floor to head level. In two group studies, group 1 with various values of Q_{in} is the most sensitive from the point of view of varying air temperature distribution along the vertical line from the foot to head level of a sedentary occupant in the room.

v.   No energy saving index which can be generally accepted has been established so far. Compared to conventional air-conditioning, the RACM is predicted to be energy saving and to provide individual thermal comfort.

vi. It is possible to create two independent temperature regions in the experimental room.

6. Acknowledgement

7. References

[1] Y. Murakami, M. Terano, K. Mizutani, Field experiments on energy consumption and thermal comfort in the office environment controlled by occupants' requirements from PC terminal, Build. Environ. 42 (2007) 17–27.

[2] ISO 7730 Moderate thermal environments – Determination of PMV and PPD indices and specification of the conditions for thermal comfort, International Organization for Standardization, Geneva. 1994.

[3] S.H. Cho, W.T. Kim, Thermal characteristics of a personal environment modules task air conditioning system: an experimental study, Energy Convers. Manag. 42 (2001) 1023–1031.

[4] Q. Zeng, J. Kaczmarczyk, A. Melikov, P.O. Fanger, Perceived air quality and thermal sensation with personalized ventilation system. Proceedings of 8th International Conference of Air Distribution in Rooms-Room Vent 2002, Copenhagen, Denmark 61–64.

[5] Melikov, A.K. Personalized ventilation, *Indoor Air,* 2004, 14, 157–167.

[6] Nielsen PV, Bartholomaeussen NM, Jakubowska E, Jiang H, Jonsson OT, Krawiecka K, Mierzejewski A, Thomas SJ, Trampczynska K, Polak M, Soennichsen M. Chair with integrated personalized ventilation for minimizing cross infection, Proceeding of Room Vent 2007, paper 1078 (2007)

[7] Nielsen PV, Barszcz E, Czarnota T, Dymalski DP, Jasiensky MA, Nowotka A, Mozer A, Wiankowska SM, Jensen RL. The influence of draught on a seat with integrated personalized ventilation, the 11th International Conference on Indoor Air Quality and Climate, Copenhagen, Denmark Paper ID: 247 (2008)

[8] J. Niu, N. Gao, M. Phoebe, H. Zuo, Experimental study on a chair-based personalized ventilation system, Build. Environ. 42 (2007) 913–925.

[9] S. Schiavon, A. Melikov, Energy saving and improved comfort by increasing air movement, Energy Build. 40 (2008) 1954–1960.

[10] S. Schiavon, A. Melikov, Energy strategies with personalized ventilation in cold climantes, Energy Build. 41 (2008) 543–550.

[11] S. Schiavon, A. Melilov, C. Sekhar, Energy analysis of the personalized ventilation system in hot and humid climates, Energy Build. 42 (2010) 699–707.

[12] B. Yang, A.K. Melikov, C. Sekhar, Ceiling mounted personalized ventilation system integrated with a secondary air distribution system – a human response study in hot and humid climate, Indoor Air 20 (4) (2010) 309 – 319.

[13] B. Yang, C. Sekhar, A.K. Melikov, Ceiling mounted personalized ventilation sytem in hot and humid climate – An energy analysis, Energy and Buildings 42 (2010) 2304 – 2308.

[14] D. Faulkner, W. J. Fisk, D.P. Sullivan, D.P. Wyon, Ventilation efficiencies of task/ambient conditioning systems with desk-mounted air supplies, Indoor Air. 9 (1999) 273–281.

[15] K.D. Huang, N.A. Tuan, K.T. Tseng, A numerical study of regional air-conditioning mechanism, Paper presented at 2008 IEEE International Conference on Sustainable Energy Technologies, 2008, Singapore.

[16] K.D. Huang, N.A. Tuan, Y.C. Shih, Energy-saving and thermal comfort studies of a regional air-conditioning mechanism. Proceedings of the Institution of Mechanical Engineers, Part A: J. Power Energy. 223 (2010) 12–33.

[17] K.D. Huang, N.A. Tuan, Numerical analysis of an air-conditioning energy-saving mechanism, Build. Simul.: Int. J. 3 (2010) 63–73.

[18] Fluent 6.3, Fluent Inc., Lebanon, NH 03766, USA, 2006.

[19] GAMbit 2.4. User guide, all volumes. Lebanon, NH 03766, USA: Fluent Inc. 2007.

[20] B.E. Launder, D.B. Spalding, The numerical computation of turbulent flows, Comput. Methods Appl. Mech. Eng. 3 (1974) 269–289.

[21] ASHRAE handbook fundamentals, ASHRAE, Inc., Atlanta, USA, Chapter 8, 2005, pp. 8.1–8.29.

[22] Thermal environmental conditions for human occupancy, ANSI/ASHRAE Standard 55–1992.

[23] Levermore, G.J. and Levermore, G. Building energy management systems: application to low-energy HVAC and natural ventilation control, E&FN Spon, London, 2000, Chapter 12, pp. 389–399.
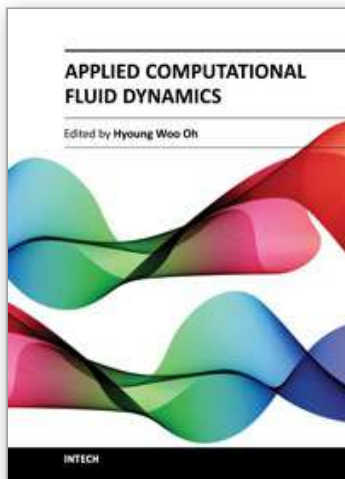
Applied Computational Fluid Dynamics

Edited by Prof. Hyoung Woo Oh

This book is served as a reference text to meet the needs of advanced scientists and research engineers who seek for their own computational fluid dynamics (CFD) skills to solve a variety of fluid flow problems. Key Features: - Flow Modeling in Sedimentation Tank, - Greenhouse Environment, - Hypersonic Aerodynamics, - Cooling Systems Design, - Photochemical Reaction Engineering, - Atmospheric Reentry Problem, - Fluid-Structure Interaction (FSI), - Atomization, - Hydraulic Component Design, - Air Conditioning System, - Industrial Applications of CFD

How to reference

In order to correctly reference this scholarly work, feel free to copy and paste the following:

Nguyen Anh Tuan, Wu-Chieh Wu and K-David Huang (2012). Study of an Individual Air-Conditioning Energy-Saving Equipment, Applied Computational Fluid Dynamics, Prof. Hyoung Woo Oh (Ed.), ISBN: 978-953-51-0271-7, InTech, Available from: http://www.intechopen.com/books/applied-computational-fluid-dynamics/study-of-an-individual-control-energy-saving-air-conditioning-system

INTECH
open science | open minds